Steady-state Photoconductivity Measurements Method for the Determination of Effective Excess Carrier Lifetime in GaSb Semiconductor

by

Shiferaw Tesema Geleta

April, 2017

Steady-state Photoconductivity Measurements Method for the Determination of Effective Excess Carrier Lifetime in GaSb Semiconductor

by

Shiferaw Tesema Geleta

Submitted in Partial fulfillment of the requirements for the degree of Master of Science in Physics in the School of Applied Natural Science at Adama Science and Technology University

Advisor

Dr. Megersa Wodajo

April, 2017

Adama, Ethiopia

ADAMA SCIENCE AND TECHNOLOGY UNIVERSITY
POSTGRADUATE PROGRAM
SCHOOL OF APPLIED NATURAL SCIENCE
APPLIED PHYSICS PROGRAM

As thesis research advisor, I hereby certify that I have read and evaluated this thesis entitled: "**Steady-state Photoconductivity Measurements Method for the Determination of Effective Excess Carrier Lifetime in GaSb Semiconductor**" prepared under my guidance by Shiferaw Tesema. I recommend that it can be submitted as fulfilling the thesis requirement.

Dr. Megersa Wodajo	_____	_____
Advisor	Signature	Date

As members of the Board of Examiners of the M.Sc. thesis Open Defense Examination, we certify that we have read and evaluated the thesis work prepared by **Shiferaw Tesema** and examined the candidate. We recommended that the thesis be accepted as fulfilling the thesis requirement for the Degree of Master of Science in Physics.

_____	_____	_____
Chairperson	Signature	Date
_____	_____	_____
Internal Examiner	Signature	Date
_____	_____	_____
External Examiner	Signature	Date

Declaration and Statement of the Candidate

This thesis has been submitted in partial fulfillment of the requirements for M.Sc. degree in physics at the ASTU. I solemnly declare that this thesis work is not submitted to any other institution anywhere for the award of any academic degree, diploma, or certificate.

Brief quotations from this thesis are allowable without special permission provided that accurate acknowledgement of source is made. Requests for permission for extended quotation from or reproduction of this manuscript in whole or in part may be granted by the head of major department or the Dean of the School of Graduate Studies when in his or her judgment the proposed use of the material is in the interests of scholarship. In all other instances, however, permission must be obtained from the author.

Name of candidate: **Shiferaw Tesema** Signature: _____

Place: **Adama Science and Technology University, Adama**

Date of Submission: **April, 2017**

Acknowledgements

First of all, I would like to thank my advisor, Dr. Megersa Wodajo, for his professional guidance and support throughout the course of my research. I like to extend my sincere thanks to him for his technical support, constructive criticism and willingness to support, effort, passion and inspiration during the completion of this thesis.

I would like to thanks also Nelson Mandela Metropolitan University laboratory for its support data of p-type epitaxial GaSb sample in this study.

Next, I am truly indebted to my wife and life partner Dame Takele for her uninterrupted love, patience and encouragement that made possible my whole dedication towards the present study. She has been a mainstay of support throughout my studies.

I would like to thank also my brothers, Shanko Tesema and Tesfaye Regasa for their giving me moral, full support and encouragement.

I would like to thank Guder Preparatory school director Milkesa Negera and vice director Yadesa Nurgi for their support in material like paper, internet service as well as mental support and ensuring a conducive environment for my research work.

I am grateful to my workmate friends Bedasa Shifera and Atrsaw Ambachew for their friendly assistance and stimulating team spirit.

Table of Contents

List of Figures

Figures **pages**

List of Abbreviations

i_{ph}	Photocurrent
V_{ph}	Photo voltage
R_{ph}	Photo resistance
V_d	Dark voltage
i_d	Dark current
R_d	Dark resistance
R_L	Load resistance
G_0	Optical generation rate
μ_n	Mobility of electron
μ_p	Mobility of hole
$\delta\sigma$	Excess of photoconductivity
α	Absorption coefficient
m_n^*	Effective mass of electrons
m_p^*	Effective mass of holes
n	Number of free electron
δn	Excess electron density
p	Number of free hole
δp	Excess hole density
σ	Conductivity
E_g	Energy band-gap of a semiconductor
E_{ph}	Photon energy
τ_n	Electron lifetime
τ_p	Hole lifetime
τ_{eff}	Effective lifetime
k_∞	Dielectric constant
R	Reflection coefficient
h	Planck's constant
λ	Wavelength of light
c	Speed of light
EHPs	Electron hole pairs
NDF	Neutral Density Filter

Abstract

In this study, the photo-response of gallium antimonide (GaSb) epitaxial films is investigated by measuring the spectral as well as injection level dependence of the steady-state photoconductivity. First, the conditions for the determination of optimum photo-signals is established by varying the load resistance connected to the sample during photoconductivity measurements. Then, the spectral dependence of the effective excess carrier lifetimes is described using the various photo-response and galvanometric measurements. The measured and theoretical effective excess carrier lifetimes were fitted using a three-layer model described using Ohm's law by considering the generation-recombination mechanisms in the deep bulk and the two under surface depleted near-surface regions on either sides of the semiconductor films. The results of the measurements revealed that the main contribution to the low injection level entire bulk photo-response mainly come from the near-surface regions, where the band to-band radiative and Auger recombination mechanisms are very low. From the simulation of the results of the excess carrier lifetime, some of the near-surface characteristics, such as the position of the surface Fermi-level, the band bending at the surface, widths of the under surface depletion layer and the surface recombination velocity, could be determined. The room temperature surface Fermi-level was found to be pinned below the mid-gap irrespective of the doping density in p-type GaSb epilayers.

1. Introduction

Semiconductor is a crystalline or amorphous solid whose electrical conductivity is typically intermediate between that of a metal and an insulator and can be changed significantly by varying the temperature or the impurity content of the material, or by illumination with light [1]. It is the foundation of modern electronic world, enormously applying in daily life products.

Elemental semiconductors include antimony, arsenic, boron, carbon, germanium, selenium and silicon. Common semiconductor compounds include gallium arsenide, gallium antimonide (GaSb), indium arsenide and indium antimonide [2]. GaSb and these related compounds are direct band-gap semiconductors high carrier mobility [3]. Thus, the common applications of these semiconductors are suitable in a variety of optoelectronic devices for both the detection and generation of electromagnetic radiation, and also in high-speed electronic devices [4]. The photo response of these materials makes it very useful in the design of a variety of device architectures, including photo detectors, resonant tunneling structures and other quantum devices. The performance of the material in this case depends on the lifetime of free charge carriers generated by the interaction of light with the material, referred to as the excess carrier lifetime [5]. In a direct band gap material, optical absorption occurs near the surface of the material whereas for a material having indirect band gap, light penetrates much deeper into the material [6].

Normally, semiconductors are relatively poor electrical conductors because they have only a small number of electrons that are free to move under a voltage. Most of the electrons are bound to their atomic lattice in the set of energy states called the valance band. But if external energy is provided, some electrons are raised to the conduction band where they can move and carry current [7].

The practical magnitudes of the dimensions of the samples are in micrometers to be compatible with the magnitudes of the parameters of the illuminating lights. The mobility of free carriers in semiconductor ranges from $10^2 cm^2 V^{-1} s^{-1}$ to $10^4 cm^2 V^{-1} s^{-1}$. The typical room

temperature mobility of electrons for most semiconductors is ranged from $10^3 cm^2 V^{-1} s^{-1}$ to $10^4 cm^2 V^{-1} s^{-1}$ and that of holes is also ranged from $10^2 cm^2 V^{-1} s^{-1}$ to $10^3 cm^2 V^{-1} s^{-1}$ [8]. The energy band gap of small direct band gap semiconductor is ranged from 0.3eV to 1.1eV like the energy bang gap of $GaSb = 0.727eV$ *and* $InAS = 0.36eV$ [9]. Bandgaps are one of the most important properties of modern semiconductors. With applications in photovoltaics, micro processing, visual display, and lighting sources, the bandgap of a semiconductor is an important property for designing and discovering new applications for semiconductors.

The discovery of the sun's light being made up of a variety of wavelengths by Isaac Newton in 1666 was the first step in the use of spectroscopy to characterize materials [10].It was not until the early 1800's that Kirchhoff discovered that each element and compound has its own unique spectrum which could be used to identify the material. When the light is shining on a semiconductor sample, if the energy of the individual photons is greater than the semiconductor band gap, then the photons can be absorbed, transferring their energy to an electron and the absorbed photon has the possibility of exciting an electron from the valence band to the conduction band [11] .The free electrons and holes produced due to this absorbed photon in the material become raise the electrical conductivity of the semiconductor. This increase is called photoconductivity and the electrical conductivity in semiconductors depends on the concentration of electrons and holes and their mobility [12]. The concentration of electrons and holes within the conduction or valence band is dependent on the light illumination as well as other properties of the material. These properties include the effective masses of electron and hole [13]. The incident photon flux density,Φ_0 is a measure of how many photons are attacking an area on the surface of the material. Photons incident on the surface of a semiconductor will be either reflected from the top surface, or will be absorbed in the material, or, failing both above processes, will be transmitted through the material. The absorption coefficient, α for a material is dependent on the wavelength of the incident light and helps to determine the amount of incident energy that is absorbed in the material. The measured photocurrent is proportional to the incident light intensity. This maximum photocurrent occurred when each incoming photon creates one electron-hole pair, which contributes to the photocurrent. As high-energy photons are

incident, an electron–hole pair is generated. The additional electrons and holes created are called excess electrons and excess holes.

Photoconductivity is an important property of semiconductors by means of which the conductivity of the sample changes due to incident radiation. The term photo-conductivity refers to a change in conductivity of a semiconductor when illuminated by photons [14]. It is an elementary process in solids and as the name suggests, it involves the generation and recombination of charge carriers and their transport to the electrodes. Photoconductivity serves as a tool to understand the internal processes or performance of the materials. The main applications of photoconductivity devices are light meters, infrared detector, TV cameras, voltage regulator, communicates and detecting ships and air crafts. Certain light sensitive crystalline semiconductors such as silicon, germanium, lead sulfide and cadmium sulfide are used as light sensors due to their photoconductivity.

When a photoconductive material was connected as part of a circuit, it functions as a resistor whose resistance depends on the light intensity [15]. In this context, the material is called a photo-resistor and also called light-dependent resistor or photoconductor. The most common application of photo-resistors is as photo-detectors, i.e. devices that measure light intensity. Some photo-detector applications in which photo-resistors are often used include camera light meters, street lights, clock radios, and infrared detectors. The high resistance of photoconductive cell in the dark is called dark resistance. The resistance of a photo resistor decreases with increasing incident light intensity. Currently the production of photovoltaic energy is constantly increasing due to power generation is reliable, it does not have any moving parts and care costs are quite cheap. Other positive advantages are: photovoltaic system is silent and it has no effect on the atmosphere (Markvart,T.1994). The term photovoltaic effect describes the generation of voltage or electric current in a semiconductor under exposure to light radiation [16]. The optical carrier generation in photovoltaic materials is based both on properties of the material and properties of the incident light.

Like common mortals, electrons and holes annihilate after being generated thermally or optically. The mechanism by which electron hole pairs annihilated is called recombination mechanism. The rate at which free carriers disappear or recombine was given by the ratio of the free carrier concentration to excess carrier lifetime [17]. In a steady-state situation the

generation and recombination rates are perfectly balanced. Electric fields and optical energy causes electron densities and velocities to be different from the equilibrium values.

The time interval through which excess carrier can stay in conduction is called excess carrier lifetime. The excess carrier lifetime is an important parameter as it characterizes the quality of the semiconductor material and hence affects the performance of the electron devices fabricated from it [18]. Therefore, for many applications, it is necessary to know the lifetime of excess carriers in the material before device processing and fabrication. High level excess carrier lifetimes are indicative of quality materials for optoelectronic devices. Processing of various semiconductor devices can also be effectively monitored and improved by systematic lifetime measurements. Therefore the carrier lifetime is the most important electronic property of semiconductor materials as a fast method to characterize the material quality [19]. In single crystalline silicon, because of its defect free structure, carriers have long lifetime. Crystalline silicon is the best example of a material with an indirect band gap, meaning that the minimum of the conduction band and the maximum of the valence band are not at the same k.

The conductivity of the semiconductor material under illumination in this study used for determine the excess carrier concentration, changes in the spectral profile of the incident photons and the total absorbed photon flux density on thin film semiconductor as allow for a determination of optical generation. In this thesis the effective lifetime is measured using Ohm's law. Also in this studying of semiconductor materials, devices and circuits, lifetime measurements would useful in gaining a better understanding of generation and recombination mechanisms.

The general objective of this study is to use steady-state photoconductivity measurements method for the determination of effective excess lifetime in semiconductors.

The specific objectives are to study:

- the method of signal current measurement using monochromator,
- the effects of load resistance (external circuit element) on the signal voltage measured using the monochromator and
- determination of excess carrier lifetime from the signal current measured using steady-state photoconductivity measurement.

This thesis divided in to the following chapters: Chapter 2 deals with the theory of, thermal equilibrium of carrier concentration, Photon absorption and free carrier generation, photoconductivity measurement, Wavelength and absorption coefficient for direct band gap and equations leading the photoconductivity of semiconductor sample before and during illumination as well as photo generation for thin film of semiconductor for the determination of effective lifetime illustrated are derived in this Sections. Chapter 3 describes the explanation systems that have been used in this work and methods of determining the effective excess lifetime in sample of semiconductor. Chapter 4 focuses on the results obtained after different methods completed. Chapter 5 presents the details of this thesis conclusion and summarize the concept of results obtained in chapter 4.

2.Review of literature

2.1. Thermal Equilibrium Properties of Semiconductors

In this section, the description of some common properties of semiconductor materials like the energies of the charge carriers and the free charge carrier concentrations will be discussed.

2.1.1 Energy Band-gap

In crystalline solids, the energy band gap between the valance band maximum and the conduction band minimum is referred to as energy band gap, $E_g = E_V - E_C$.The band-gap energy of a semiconductor defines its optical absorption threshold for the photoelectric effect. When supra-band-gap light is absorbed by a semiconductor, charges move between the valence and conduction bands [20].

A contraction of the crystal lattice with decreasing temperature usually leads to a strengthening of the interatomic bonds and an associated increase in the band gap energy. The first empirical relation for the band gap shift with temperature was developed by Varshni *et al* [21]. The temperature dependence of the energy band-gap, $E_g(T)$ is related by the relation [22, 23] :

$$E_g(T) = E_g(0) - \frac{\alpha T^2}{T + \beta} \qquad (1)$$

where α and β are constants chosen to obtain the best fit to experimental data and $E_g(0)$ is the limiting value of the band at zero Kelvin.

Direct band gap materials do not involve phonons (lattice vibrations) in electron band-to-band transitions [24]. The absorption coefficient α, is a property of a material which defines the amount of light it absorbs [25]. The wavelength-dependent value of α determines how far the light enters the semiconductor. The absorption coefficient of a semiconductor material at a given wavelength determines the spatial region in which most of the light is absorbed. For high absorptivity, most of the light is absorbed close to the semiconductor surface. Semiconductors with direct energy gap are generally characterized by; a high absorption coefficient in the relevant energy range for photovoltaic, most of the sunlight is absorbed within a small range beneath the surface and possibility to fabricate thin film solar

cells. Whereas indirect band semiconductors need more material to absorb most of the sunlight; (Si, Ge, GaP) thicker layers are needed; higher material costs and increased demands on purity increase prize [26].

2.1.2 Thermal Equilibrium Carrier Concentration

The concentrations of electrons and holes in a semiconductor are determined by many factors including the bandgap and band structure of the semiconductor, the types and concentrations of the impurities doped in the semiconductor, temperature and any external disturbances to the semiconductor [27]. The term equilibrium is used to describe the unperturbed state of a system, to which no external voltage, illumination, mechanical stress, or other perturbing forces are applied. Therefore, thermal equilibrium concentration of electron and hole in conduction and valance bands are independent of time. In thermal equilibrium electron-hole pairs are constantly being formed and destroyed. For a non-illuminated semiconductor in thermal equilibrium, the concentration of electrons in the conduction band is $n = n_0$ and holes in the valence band $p = p_0$. These concentrations remain constant due to the equilibrium between generation and recombination processes. The thermal equilibrium electron concentration, n_0 in the conduction band and thermal equilibrium hole concentration, p_0 in the valence band for the non-degenerate semiconductor case can be simplified to [28]:

$$n_0 = N_C \exp\left(-\frac{E_C - E_F}{k_B T}\right), \qquad p_0 = N_V \exp\left(-\frac{E_F - E_V}{k_B T}\right) \tag{2}$$

where N_C and N_V are the density of states in the conduction and the valence bands, respectively and described as:

$$N_C = 2\left(\frac{2\pi m_n^* k_B T}{h^2}\right)^{3/2} \quad \text{and} \quad N_V = 2\left(\frac{2\pi m_p^* k_B T}{h^2}\right)^{3/2}, \tag{3}$$

where m_n^* and m_p^* are effective mass of electrons in conduction band and holes in the valance band, respectively. The intrinsic carrier cconcentration is given by [29]:

$$n_i = \sqrt{N_C N_V} \exp\left(-\frac{E_g}{2k_B T}\right), \tag{4}$$

and the intrinsic energy level is also given as [30]:

$$E_i = \frac{E_V + E_C}{2} + \frac{3}{4} k_B T \ln\left(\frac{m_p^*}{m_n^*}\right), \tag{5}$$

where E_V and E_C are the respective energies at the valence band maximum and conduction band minumum. The bulk fermi level positon, E_{BF} is also given by [31, 32]:

$$E_{BF} = E_i - k_B T \ln\left(\frac{p_0}{n_i}\right). \tag{6}$$

For a p-type semiconductor doped with a very high concentration shallow acceptor, relations in Eqn. (2) above take the form [33]:

$$n_0 \approx \frac{n_i^2}{N_a}, \qquad p_0 \approx N_a, \tag{7}$$

where N_a is the acceptor concentration.

2.1.3 Near Surface Depletion layer at Thermal Equilibrium

When an electric field **E** is applied to the material, the band energies become a function of position. The variation of E_C and E_V with position is referred to as band bending. The description of the band bending , $E_S(x)$ at any location x *in* the depletion region is enables to evaluate the thermal equilibrium free carrier densities at any point in the depletion region. By considering the energy band bending, E_S at the surface:

$$E_S = E_{SF} - E_{BF,} \tag{8}$$

where E_{SF} is the surface Fermi pinning position above the valence band maximum (VBM) approximaetly at 300 meV irrespective of the doping level, the thermal equilibrium carrier densities at the surface are given by [34, 35]:

$$p_{0S} = N_a \exp\left(-\frac{E_S}{k_B T}\right) \qquad \text{and} \qquad n_{0S} = N_a \exp\left(\frac{E_S}{k_B T}\right). \tag{9}$$

and the width, b_1 of the depletion layer is given by:

$$b_1 \approx \sqrt{\frac{2\epsilon E_S}{e^2 N_a}}, \tag{10}$$

where ϵ is the permittivity of the material. The average thermal equilibrium carrier concentration in the entire depletion layer is given by:

$$\bar{p}_{01} = \frac{2L_D^2}{b_1^2} N_a \left[1 - \exp\left(-\frac{b_1^2}{2L_D^2}\right)\right], \tag{11}$$

where L_D is called the *Debye length* given by:

$$L_D = \sqrt{\frac{\epsilon k_B T}{e^2 N_a}}. \tag{12}$$

2.2 Photo-response of semiconductors

The interaction of light with matter can be viewed macroscopically as consisting of four components: incident, reflected, transmitted and absorbed (or scattered) components. Using these components of photons one can describe several properties of the material. The reflectivity and absorption depth and the scattering depth of photons in the material depend on the material and the photon energy. The photo-response of the material hence can be measured through the change in the photoconductivity due to the absorbed photons. In this section, the concept of photon absorption in thin film and free carrier generation in semiconductor materials are described.

2.2.1 Photon Absorption in thin film sample

Free carrier generation from light absorption only occurs with photons with energies greater or equal to the band gap, E_g (or $h\upsilon \geq E_g$), where h is the Planck's constant and υ is the frequency of the absorbed photon by the semiconductor. When a semiconductor is illuminated by a photon of energy greater than its energy band gap ($h\upsilon > E_g$), electron-hole pairs are generated in the semiconductor [36]. In the case of a pure semiconductor, Photons with an energy less than E_g, however, cannot be absorbed and the semiconductor is transparent for light with wavelengths longer than $\lambda = \frac{hc}{E_g}$, or it will not be enough to excite an electron from the valence band to the conduction band and it will pass through the semiconductor without being absorbed [37]. While the photo-generated carriers exist in their respective bands, they are free to contribute to the conductivity of the material. The electron-hole pairs generated by photon absorption are known as photo-generated carriers.

The rate of photon absorption in a sample depends on intensity of incident photon flux density Φ_0, the reflectivity of the illuminated sample R, the absorption coefficient α and the

thickness of the sample b. Figure 1 illustrates a double sided thin film of GaSb sample with thickness b illuminated by a source with incident of photon flux density Φ_o.

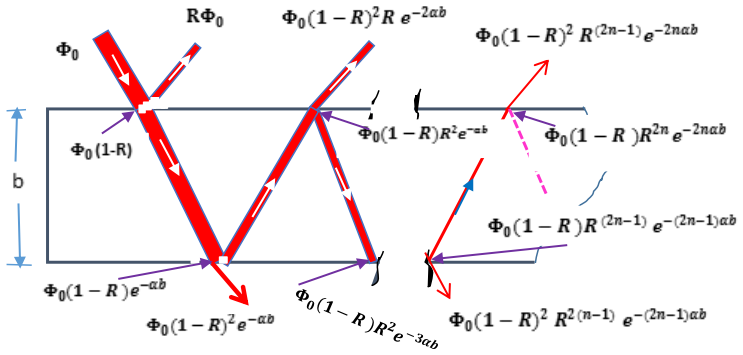

Figure 1: Absorption of photon in thin film semiconductor

The expressions and the arrows in the Figure 1 describe the incident, reflected and transmitted rays at the boundaries of the sample. When the incident of photon flux density meets the sample of thin film semiconductor; some photons are absorbed, reflected and some are transmitted. The processes of reflection, transmission and absorption are repeated many times until all the photons are absorbed by the material and transmitted through the surfaces. After n^{th} reflection, the total reflected or scattered photon flux density (Φ_R) through the top surface is given as:

$$\Phi_R = \Phi_0 R + \Phi_0 (1-R)^2 \sum_{n=1}^{\infty} R^{2n-1} e^{-2n\alpha b}$$

or

$$\Phi_R = \Phi_0 R \left(\frac{1 + (1-2R)e^{-2\alpha b}}{1 - R^2 e^{-2\alpha b}} \right), \qquad (13)$$

where R is the reflection coefficient of the surface, Φ_0 is incident photon flux density, b is thickness of the sample and α is the absorption coefficient. The value of the absorption coefficient is determined using its dependence on the photon energy, analyzed by Bardeen *et al* [38, 39] as:

$$\alpha(\omega) = \frac{2^{\frac{2}{3}} m_n e^2}{3\hbar^2 \sqrt{k_\infty}} \left(\frac{m^*{}_n m^*{}_p}{m_n (m^*{}_n + m^*{}_p)} \right)^{\frac{3}{2}} \left(1 + \frac{m_n}{m^*{}_n} + \frac{m_n}{m^*{}_p} \right) \left(\frac{\hbar\omega - E_g}{m_n c^2} \right)^{\frac{1}{2}}, \qquad (14)$$

where, $\hbar$ is the reduced Plank's constant, e is the elementary charge and c is the speed of light. Large values of α indicate strong absorption and *vice versa*. The incident photon flux

density Φ_0 is a measure of how many photons are incident on the semiconductor material [40]. The light intensity which is a measure of the flux of photons in the optical beam decreases through the sample as the photons are absorbed [41, 42].

The total photon flux density (Φ_T) transmitted or scattered through the bottom surface is also given by:

$$\Phi_T = \Phi_0(1-R)^2 \sum_{n=1}^{\infty} R^{2(n-1)} e^{-(2n-1)\alpha b}$$

or

$$\Phi_T = \frac{\Phi_0(1-R)^2 e^{-\alpha b}}{1-R^2 e^{-2\alpha b}}. \tag{15}$$

The total photon flux density absorbed in the sample is given by the difference between the incident photon flux density and the sum of the photon flux densities transmitted and reflected of the sample, Eqns. (13) and (15). This is mathematically described as:

$$\Delta\Phi = \Phi_0 - (\Phi_R + \Phi_T)\,. \tag{16}$$

Then, by substituting Eqns. (13) and (15) into Eqn. (16) the total photon flux density simplified to:

$$\Delta\Phi = \Phi_0(1-R) - \Phi_0\,(1-R)^2[R^{-1} + R^{-2}\,e^{\alpha b}] \sum_{n=1}^{\infty} R^{2n} e^{-2n\alpha b}. \tag{17}$$

Since $R < e^{\alpha b}$, we have:

$$\Delta\Phi = \frac{\Phi_0(1-R)(1-e^{-\alpha b})}{1-Re^{-\alpha b}}. \tag{18}$$

Then, the absorption rate, G_0 in the entire sample of thickness can be determined from the ratio of the total absorbed photon flux density $\Delta\Phi$ the sample to the thickness b of the thin film semiconductor materials:

$$G_0 = \frac{\Delta\Phi}{b} = \frac{\Phi_0(1-R)(1-e^{-\alpha b})}{b(1-Re^{-\alpha b})}. \tag{19}$$

Using the same method, the respective photon absorption rates in the upper depletion layer 1, G_{01} the quasi neutral region, G_{02} and the bottom depletion layer 2, G_{03} can be described as:

$$G_{01} = \frac{\Phi_0(1-R)(1-e^{-\alpha b_1})\left(1+Re^{-\alpha(2b-b_1)}\right)}{b_S(1-R^2e^{-2\alpha b})}, \tag{20}$$

$$G_{02} = \frac{\Phi_0(1-R)e^{-\alpha b_1}\left(1-e^{-\alpha(b-2b_1)}\right)}{(b-2b_1)(1-Re^{-\alpha b})}, \quad (21)$$

and

$$G_{03} = \frac{\Phi_0(1-R)e^{-\alpha(b-b_S)}(1-e^{-\alpha b_S})(1+Re^{-\alpha b_S})}{b_S(1-R^2e^{-2\alpha b})}. \quad (22)$$

2.2.2 Description of photo conductivity using Ohm's law

When light is absorbed by a semiconductor sample, the density of free electrons and holes increases and raises its electrical conductivity. In other hand, the increase in conductivity is due to the increase in the densities of n and p charge carriers compared to their values at thermal equilibrium. Therefore, the conductivity of semiconductors is proportional to the concentration of carriers within the semiconductor. The photoconductivity of semiconductor can be determined applying equation of Ohm's law [43]:

$$\mathbf{J} = \mathbf{J}_n + \mathbf{J}_p. \quad (23)$$

The respective current densities of electrons and holes are given by:

$$\mathbf{J}_{\mathrm{n}} = -en\mathbf{v}_{dn} \quad \text{and} \quad \mathbf{J}_{\mathrm{p}} = ep\mathbf{v}_{dp}, \quad (24)$$

where $\mathbf{v}_{dn}$ and $\mathbf{v}_{dp}$ are drift velocities of electrons and holes, respectively and n and p are the respective non thermal equilibrium electron and hole densities. The drift velocities of the carriers are also directly proportional to the electric field strength, $\mathbf{E}$ applied to the system:

$$\mathbf{v}_{\mathrm{dn}} = -\mu_n\mathbf{E} \quad \text{and} \quad \mathbf{v}_{\mathrm{dP}} = \mu_p\mathbf{E}, \quad (25)$$

where μ_n and μ_p are constants called the electron and hole mobilities, respectively. Mobility is a measure of how easily the carriers can move through a semiconductor material. Drift velocities $\mathbf{v}_{\mathrm{dn/p}}$ is drift velocity which is the basic mechanisms to transport of the motion of electric charged particle in response to an electric field. The negative sign in Eqn. (25) shows that the electron's velocity is in the opposite direction to that of the electric field strength. In an electric field the force acts on the charged particles in a semiconductor, which accelerates the positively charged holes in the direction of the electric field and the negatively charged electrons in the direction opposite to the electric field. Therefore, electrons and holes move

in opposite directions resulting in a photocurrent. Taking into account relations (25) and (24) along with relation (23) yields:

$$\mathbf{J} = e(n\mu_n + p\mu_p)\mathbf{E} = \sigma\,\mathbf{E}, \tag{26}$$

where, $\sigma = \sigma_n + \sigma_p$ is the non-thermal equilibrium conductivity of semiconductor material due to the contribution from both electrons and holes in which the respective contribution of conductivities from electrons and holes are given as:

$$\sigma_n = en\mu_n \quad \text{and} \quad \sigma_p = ep\mu_p. \tag{27}$$

At thermal equilibrium; conductivity of semiconductor derived by applying Ohm's law is given as:

$$\sigma_{n0} = en_0\mu_n \quad \text{and} \quad \sigma_{p0} = ep_0\mu_p. \tag{28}$$

The conductivity of semiconductor at thermal equilibrium, σ_0 due to hole and electron is given by:

$$\sigma_0 = e(\mu_n n_0 + \mu_p p_0). \tag{29}$$

If light is shone on the semiconductor materials, the electrons and holes concentrations increases by δn and δp, respectively. The photo-generated electrons and holes change the total electron and hole concentrations in the semiconductor to new values n and p, respectively given by:

$$n = n_0 + \delta n \quad \text{and} \quad p = p_0 + \delta p, \tag{30}$$

where δn and δp are the respective electron and hole densities generated by illumination. The increase in the total photoconductivity, $\delta\sigma$ due to illumination is obtained by subtracting the conductivity of semiconductor at thermal equilibrium, σ_0 in relation (28) from the non-thermal equilibrium conductivity in relation (26):

$$\delta\sigma = e(\mu_n\delta n + \mu_p\delta p). \tag{31}$$

Hence, the excess electron-hole pairs generated during illumination thus created contribute to the conductivity of the semiconductor sample. In the absence of carrier trap $\delta n = \delta p$, so that:

$$\delta\sigma = e(\mu_n + \mu_p)\,\delta n. \tag{32}$$

2.2.3 Free Carriers Generation-Recombination Mechanisms

Recombination of charge carriers is the opposite of generation of charge carriers, representing mechanisms that reduce the excess charge density. When there is generation of charge carriers, it is always balanced at steady-state by the recombination of charge carriers. Recombination of charge carriers takes place both in the bulk and at the surface of a semiconductor. In deriving our recombination model, it has been assumed that the semiconductor is non-degenerate [44, 45].

Excess carrier lifetime is the average amount of time the carriers spends in the conducting state before recombination. The lifetime of charge carriers is one of the important parameters to characterize a material because, it plays a critical role in determining the semiconductor device parameters. Carrier lifetime is dependent upon a number of quantities and conditions which are characteristic in the nature of semiconductor materials and the recombination process. These quantities and conditions include excess carrier density, the type of light source, sample thickness and temperature [46, 47]. The basic method to measure the lifetime depending on the way that an excess of carriers (electrons and holes) is created in the semiconductor is using the expression for the balance between generation and recombination to calculate the lifetime. This constitutes the steady state condition [48, 49].

The lifetime for the respective excess electrons and holes τ_n and τ_p in terms of the recombination rate of excess carriers, U are given by [50] :

$$\tau_n = \frac{\delta n}{U} \qquad \text{and} \qquad \tau_p = \frac{\delta p}{U}. \tag{33}$$

If one photon ejects one electron-hole pair during illumination, the photon absorption, G_0 can be considered as equal to free carriers' generation rate, so that at steady state $U = G_0$. Hence, the steady state excess carrier lifetimes Eqn. (33) can be rewritten as:

$$\tau_n = \frac{\delta n}{G_0} \qquad \text{and} \qquad \tau_p = \frac{\delta p}{G_0}. \tag{34}$$

Optically generated charge carriers can recombine in three different ways in the bulk of the materials. These are:

1) *Radiative recombination*: which is the opposite of optical generation of charge carriers. It occurs when the energy of the excited electron is emitted by the formation of a photons

during the annihilation of an electron-hole pairs. The steady state radiative excess carrier lifetime is given by:

$$\tau_R = \frac{\tau_{R0}}{1 + C_R \tau_{R0} \delta n}, \tag{35}$$

where C_R is called carriers capture coefficient and τ_{R0} is a time constant given by:

$$\tau_{R0} = \frac{1}{C_R(n_0 + p_0)}. \tag{36}$$

For a low injection system when $1 \gg C_R \tau_{R0} \delta n$ in relation (35), we have:

$$\tau_R = \tau_{R0}. \tag{37}$$

For high injection system when $1 \ll C_R \tau_{R0} \delta n$, we get:

$$\tau_R = \frac{1}{C_R \delta n}. \tag{38}$$

2) *Auger recombination*: in which the excess energy of the carriers is transferred as excess kinetic energy to another charge carrier. The steady state Auger recombination lifetime for excess carriers is given by:

$$\tau_A = \frac{\tau_{A0}}{1 + \tau_{A0}(k_A \delta n + C_A \delta n^2)}, \tag{39}$$

where C_{pa} and C_{na} are Auger capture coefficients for free holes and electrons, respectively and

$$\tau_{A0} = \frac{1}{C_{pa}(p_0^2 + 2n_i^2) + C_{na}(n_0^2 + 2n_i^2)}, \qquad C_A = C_{pa} + C_{na},$$

$$k_A = C_{pa}(2p_0 + n_0) + C_{na}(2n_0 + p_0).$$

The low injection level Auger excess carrier lifetime when $1 \gg \tau_{A0}(k_A \delta n + C_A \delta n^2)$ is:

$$\tau_A = \tau_{A0}. \tag{40}$$

The corresponding high injection level is:

$$\tau_A = \frac{1}{C_A \delta n^2}. \tag{41}$$

3) *Shockley-Read-Hall* (SRH) *recombination*: in which the excess energy is dissipated as heat or phonon during the recombination process. At the recombination center:

$$\tau_{SRH} = \frac{\tau_{n0}(2p_0 + \delta n) + \tau_{p0} \delta n}{p_0 + \delta n}, \tag{42}$$

where τ_{n0} is the minimum SRH lifetime for free electron when all the localized states are empty and τ_{p0} is the minimum SRH lifetime for free holes when all the localized states are occupied by electrons.

For a system under low injection level:

$$\tau_{SRH} \approx 2\tau_{n0}. \tag{43}$$

For a system under high injection level τ_{SRH} is simplified to:

$$\tau_{SRH} \approx \tau_{n0} + \tau_{p0}. \tag{44}$$

The effective excess carrier lifetime in the bulk, τ_{b} is determined from the relation:

$$\frac{1}{\tau_{\mathrm{b}}} = \frac{1}{\tau_{\mathrm{R}}} + \frac{1}{\tau_{\mathrm{A}}} + \frac{1}{\tau_{\mathrm{SRH}}}. \tag{45}$$

Since the three layers with different carrier concentrations as discussed in section 2.1.3 and at the end of section 2.2.1, the excess carrier lifetimes also vary in these regions. The best way to deal with this situation is to apply Ohm's law for the three parallel currents flowing in the sample when the field is applied. Consider, three respective signal currents δi_1, δi_2 and δi_3 flowing in layer1, layer2 and layer3. The total photo signal current in the bulk is hence:

$$\delta i = \delta i_1 + \delta i_2 + \delta i_3. \tag{46}$$

This can be described in terms of the current densities as:

$$\delta jA = \delta j_1 A_1 + \delta j_2 A_2 + \delta j_3 A_3, \tag{47}$$

where A_1, A_2 and A_3 are the areas of layer1, layer2 and layer3, respectively. Since all the layers have the same width and the applied field is the same across the entire sample, Eqn. (47) is simplified to:

$$\delta\sigma = \frac{(\delta\sigma_1 + \delta\sigma_3)b_1 + \delta\sigma_2\, b_2}{b}, \tag{48}$$

where b_2 is thickness of layer 2, b_1 and b_3 are width of depletion layer 1 and 3 respectively. Relation (48) takes into account that, both the depletion layers 1 and 2 have the same thicknesses. Upon applying relation (32) to the conductivities of each layer in relation (48), we get:

$$\delta n = \frac{(\delta n_1 + \delta n_3)b_1 + \delta n_2\, b_2}{b}. \tag{49}$$

Again, applying relation (34) to relation (49) gives the entire bulk excess carrier lifetime, τ_{beff} as:

$$\tau_{\text{beff}} = \frac{b_1(G_{01}\tau_{1\text{eff}} + G_{03}\tau_{3\text{eff}}) + b_2 G_{02}\tau_{2\text{eff}}}{bG_0}. \tag{50}$$

For a system under low injection level, $\tau_{1\text{eff}} = \tau_{3\text{eff}}$, so that:

$$\tau_{\text{beff}} = \frac{b_1(G_{01} + G_{03})\tau_{1\text{eff}} + b_2 G_{02}\tau_{2\text{eff}}}{bG_0}. \tag{51}$$

Recombination of free carriers also takes place at the surface of the semiconductor. The excess carrier lifetime due to recombination at the surface is given by:

$$\tau_S = \frac{b}{2S}, \tag{52}$$

where b is thickness of the sample and S is a parameter called surface recombination velocity which is related to the energy of the surface state at the recombination center for p-type material as:

$$S = \frac{S_{n0}S_{p0}(p_{0S} + \delta n)}{S_{p0}(2p_{0S} + \delta n) + S_{n0}\delta n}, \tag{53}$$

where p_{0S} and n_{0S} the thermal equilibrium carrier concentrations at the surface discussed in relation (9); S_{n0} and S_{p0} are the surface electron and hole recombination velocities when the surface states are empty and filled by electrons, respectively.

For surface under low injection level:

$$S = \frac{S_{n0}}{2}. \tag{54}$$

For surface under high injection level:

$$S = \frac{S_{n0}S_{p0}}{S_{p0} + S_{n0}}. \tag{55}$$

The effective excess carrier lifetime in the entire sample is given by the combined effects of relations (51) and (52) as:

$$\tau_{\text{eff}} = \left(\frac{1}{\tau_{\text{beff}}} + \frac{1}{\tau_S}\right)^{-1} \tag{56}$$

or

$$\tau_{\text{eff}} = \left(\frac{bG_0}{b_1(G_{01} + G_{03})\tau_{1\text{eff}} + b_2 G_{02}\tau_{2\text{eff}}} + \frac{2S}{b}\right)^{-1}. \tag{57}$$

3.Materials and Methods

This topic presents the experimental procedures, the apparatus used in the measurements of excess carrier lifetime and the techniques for the fitting of the theoretical results with the experimental values. The first section describes the steady-state photoconductivity measurement set-ups and the experimental procedure followed. The third section presents the effect the circuit properties have on the measured signal, followed by a section describing the determination of the effective excess carrier lifetime from the photoconductivity measurements.

3.1 Apparatus and setups

Figure 2 depicts phase-sensitive system for photoconductivity measurement. The main components are a lock-in amplifier, a digital multi-meter, a light source of 100 W tungsten halogen lamp, diffraction gratings for separating photons with different energies. To determine the incident photon flux densities, commercial Si and GaAs photo-detectors were used to calibrate the spectrum across the 0.4 µm to 2.6 µm wavelength range. Neutral density filters were used to vary the illumination intensity. The incident lights were modulated using a mechanical chopper and the ac photo-signals were phase-sensitively separated from the dark current using a lock-in amplifier. For the best detection of small signals, the load resistance was adjusted to match the sample resistance.

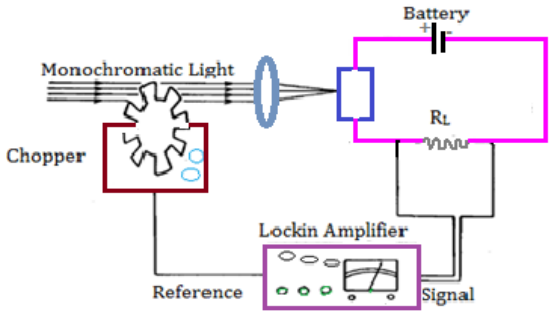

Figure 2: Phase-sensitive system for photoconductivity measurement

3.2 Sample details and experimental procedures

The samples used in this study were p-type epitaxial GaSb grown in Nelson Mandela Metropolitan University (NMMU) laboratory by metalorganic vapor phase epitaxy (MOVPE) on semi-insulating (001) GaAs substrate. The layer thicknesses of the samples were varied between 1.6 µm and 7.4 µm.

For photoconductivity measurements, 2 mm by 5 mm sections were cleaved and Ohmic contacts fabricated on the narrow ends using indium solder or silver epoxy. The fitting was performed mainly by varying the band bending at the surface (to adjust b_1) until the theoretical and the experimental excess carrier lifetimes coincided. In order to prevent photoelectric contributions from the electrodes, the contacts were masked. For injection level dependent photoconductivity measurements, the photon flux densities were varied using neutral density filters.

3.3 Principles of Measurements of the Photoconductivity

Consider a simple circuit that contains a voltage source output voltage V_0 connected in series with a semiconductor sample under illumination with photo-resistance R_p and an external (load) resistor of resistance R_L as shown in Figure 3. During a steady-state photoconductivity measurement, photo-generated carriers within the sample drift along a current path by an externally applied electric field.

The incident photon flux density of the illumination was determined using the following relation:

$$\Phi_0 = \frac{I}{h\upsilon}, \tag{58}$$

where h is Planck's constant, υ the frequency of the illumination, and I the intensity of the illumination calculated using a photodiode and and the relation:

$$I = \frac{\Delta i_p}{A\Re}, \tag{59}$$

where Δi_p is the photodiode signal current, A area of the photodiode and $\Re$ is the responsivity of the photodiode in ampere per watt (A/W).

Illumination affects only the resistance of the sample and does not affect the resistance of the load, R_L. However, the change in the resistance of the sample due to illumination can affect the voltages drop in both the sample and the load resistor. The change in the resistance of the sample can be determined by evaluating the difference between the voltages with and without illumination [51]. Since the source voltage is not affected by illumination, the sum of the sample voltage and the load voltage remains constant before and after illumination. The total voltage during illumination is hence given by:

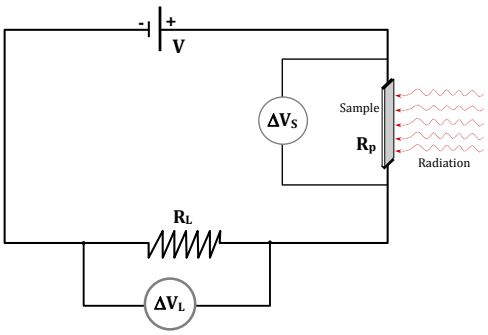

Figure 3: A simple circuit used for photoconductivity measurements.

$$V_0 = V_p + V_L = i_p(R_p + R_L), \tag{60}$$

where the respective sample and load voltages V_p and V_L during illumination are given by:

$$V_p = i_p R_p \quad \text{and} \quad V_L = i_p R_L \tag{61}$$

and i_p is the circuit current during illumination called *photo-current*. Hence, the photo-current as a function of photo resistance and load resistance can be written as:

$$i_p = \frac{V_0}{R_p + R_L} \tag{62}$$

Before illumination, the circuit voltage is given in terms of the sample dark voltage, V_d and the load voltage before illumination, V_{L0} as:

$$V_0 = V_d + V_{L0} = i_d (R_d + R_L). \tag{63}$$

The two voltages V_d and V_{L0} can be written in terms of the dark current, of the circuit, I_d as:

$$V_d = I_d R_d, \quad V_{L0} = I_d R_L, \tag{64}$$

where R_d is called the dark resistance of the sample. The dark current is expressible as function of dark and load resistance as:

$$i_d = \frac{V_0}{R_d + R_L}. \tag{65}$$

The signal response or the change in voltage of the sample by illumination is determined by taking the difference between the photo-voltage and dark voltage of the sample. Consequently, taking the difference between Eqns. (60) and (63) yields:

$$\Delta V_s \;=\; -\Delta V_L \;= -R_L \Delta i, \tag{66}$$

where

$$\Delta V_s \;=\; V_p - \; V_d \,, \qquad \Delta V_L = V_L - V_{L0} \qquad \text{and} \qquad \Delta i \;=\; i_p - \; I_d. \tag{67}$$

Substitution of Eqns. (65) and (62) into Eqn. (67) gives:

$$\Delta i \;=\; V_o \left(\frac{\Delta R_p}{(R_p \;+\; R_L)(R_d \;+\; R_L)} \right). \tag{68}$$

Taking into account Eqn. (68) along with Eqn. (66) yields:

$$\Delta V_s \;=\; -\; R_L V_0 \left(\frac{\Delta R_p}{(R_p \;+\; R_L)(R_d \;+\; R_L)} \right), \tag{69}$$

where

$$\Delta R_p = R_d \; - R_p \tag{70}$$

is the change in the sample resistance during illumination. For low injection level system $R_p \;\approx R_d$, so that Eqn. (69) can be rewritten in the form:

$$\left| \frac{\Delta V_s}{\Delta R_p} \right| \;=\; \frac{V_0 R_L}{(R_d \;+\; R_L)^2}. \tag{71}$$

A close examination of relation (71) reveals that, the signal has a strong dependence on the load resistance. The signal voltage diminishes at very small and large values of the load resistance, R_L. In order to get maximum signal, R_L has to be optimized to:

$$R_L = R_d. \tag{72}$$

The value of load resistance R_L is optimized in order to obtain the maximum photo response. The photo-conductivity of the material due to illumination is:

$$\delta\sigma = \; \frac{\ell}{A} \left(\frac{1}{R_p} - \frac{1}{R_d} \right) = \; \frac{\ell}{A} \left(\frac{\delta R_p}{R_p R_d} \right), \tag{73}$$

where ℓ is the length and A the cross-sectional area of the sample. For a system under low injection level, the photo-conductivity has very small value:

$$\delta\sigma = \; \frac{\ell}{A} \left(\frac{\delta R_p}{R_d^2} \right). \tag{74}$$

Equating relations (68) and (74) also gives the low injection level photo-conductivity to be:

$$\delta\sigma = \; \frac{\ell}{V_0} \left(1 \; + \; \frac{R_L}{R_d} \right)^2 \delta j_p, \tag{75}$$

where δj_p is the signal current density in the sample given by:

$$\delta j_p = \frac{\delta i_p}{A}. \tag{76}$$

The density of the excess carrier generated due to illumination can be obtained by equating relations (32) and (75) as:

$$\delta n = \frac{\ell}{e\mu V_0}\left(1 + \frac{R_L}{R_d}\right)^2 \delta j_p, \tag{77}$$

where

$$\mu = \mu_n + \mu_p. \tag{78}$$

3.4 Principles of Measurements of Effective Excess Carrier lifetime

Assuming that one incident photon generates one electron-hole pair, the steady state (generation rate is equal to recombination rate) free carrier concentration, δn is related to the generation rate, G_0 as:

$$\delta n = G_o \tau_{\text{eff}}, \tag{79}$$

where τ_{eff} is the effective excess carrier lifetime. Taking into account relation (77) along with relation (79) the effective excess carrier lifetime in the entire sample to be:

$$\tau_{\text{eff}} = \frac{\ell}{e\mu V_0}\left(1 + \frac{R_L}{R_d}\right)^2 \frac{\delta j_p}{G_0}. \tag{80}$$

If $R_L = R_d$ as in relation (72) above, we have:

$$\tau_{\text{eff}} = \frac{4\ell}{e\mu V_0}\frac{\delta j_p}{G_0}. \tag{81}$$

The effective excess carrier lifetime in Eqn. (81) is the effect of both the entire bulk and the surfaces of the sample discussed in relation (57).

4.Results and Discussion

The effective excess carrier lifetimes described in relations (57) and (81) the combined is predicted to be in the order nano-seconds and constant for low injection levels. However, the result of the excess carrier lifetime obtained from the steady-state photoconductivity measurements revealed that the lifetime strongly decreases with increasing injection level in the lower injection regimes ($\delta n < p_0$). This inconsistency between the expected and measured behaviors was resolved by M. W. Shura *et al.* using a two-layer model to describe the photoconductive response of bulk GaSb samples [52]. In order to resolve the discrepancy between the measured lifetimes and the theoretical predictions, they formulate a mathematical description of two-layer model to describe the experimentally obtained carrier lifetimes.

In this study, the mathematical descriptions of three-layer model discussed in chapter 2 above were formulated to describe the experimentally obtained carrier lifetimes in GaSb thin films. The excess carrier lifetime equations derived using the three-layer system in chapter 2 allow us to relate the expected bulk lifetime to various experimental factors, such as the effects of the external circuit, the spectral effect and the excitation power of the illumination used.

4.1 Effect of external circuit on the photo-signal

The variation of the photo-signal with the external circuit element is described by varying the resistance of the load resistor as equation (71). Figure 4 depicts the variation of the photo-signal with load resistance for a GaSb sample of dark resistance 500 Ω. The photo-signal diminishes at very small and large values of the load resistance. As can be seen from Figure 4, maximum signal is obtained for a load resistance equal to the sample's dark resistance. Therefore, in order to collect the optimum signal voltage during the low injection level photoconductivity measurement, the load resistance should be adjusted to match the sample resistance. It is very difficult to get photo-signal when the load resistance is much less than the sample resistance. The load resistance can be

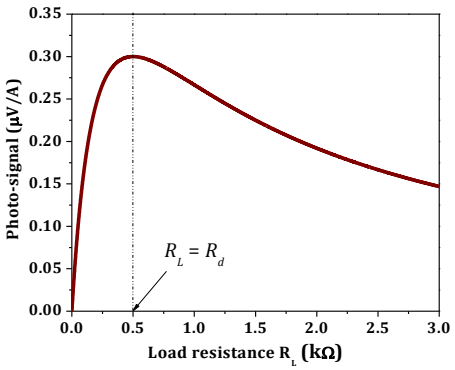

Figure 4: Variation of the photo-signal with load resistance for a GaSb sample of dark resistance 500 Ω.

adjusted to match the sample resistance when the photoconductivity measurement is performed at fixed temperature. However, the detection of photo-signal can be very difficult when the temperature dependence of photo-conductivity measurement is performed, since the sample resistance in the cryostat can be much exceeding the load resistance.

4.2 Spectral dependence of excess carrier lifetimes

The spectral variation of the steady-state photoconductivity measurements were performed by varying the excitation wavelength. The thermal equilibrium majority carrier concentrations and mobilities were obtained from the Hall Effect measurements. The quantities extracted from Hall measurements are the electron mobility, typically 10^4 $cm^2V^{-1}s^{-1}$ and 3×10^3 $cm^2V^{-1}s^{-1}$ for holes. The carrier concentrations obtained in this case are from 10^{17} cm^{-3} and 10^{18} cm^{-3}. The incident photon flux density is determined using the steady-state photoconductivity measurements of the photo-detectors in Eqns. (58) and (59). The photon absorption rate (or the excitation rate) in each layer could be estimated using the known absorption spectrum along with relations (20) to (22). The photon flux density dependence of the change in the conductivity of the sample due to illumination ($\delta\sigma$) and the net photo-generated carrier concentration (δn) was determined using relations (75) and (77). The signal current is also determined using relation (66) from the signal voltages obtained using different illuminations.

Figure 5 illustrates the spectral dependence of low injection level and relatively high injection level (a) incident and absorbed photon flux densities for p-type GaSb epilayer with room temperature carrier concentration 10^{17} cm^{-3} and mobility 700 $cm^2V^{-1}s^{-1}$ and (b) responsivity of the photo-detectors for the incident photon flux density. The level of the incident photon flux density was controlled by inserting different neutral density filters. As it can be seen from Figure 5 (a), all the incident and the absorbed photon flux densities from tungsten halogen lamp have minimum values at low and high wavelengths, reaching maximum near 1.1 μm. The sample (absorbed) signal drops sharply at the absorption edge and the responsivity increases with increasing the wavelength.

The sample dark resistance (R_d) was 690 Ω and the load resistance (R_L) was selected to be 830 Ω to get close to an optimum signal, as suggested in Figure 4. The dark bias voltage was 2.5 V; the thickness, the width and the length of the sample used were 4.7 μm, 1.5 mm

and 7.0 mm, respectively. The responsivity of the sample to the illumination can be determined as a function of the wavelength using relation (59) by dividing the photo-generated current by the illumination light power. Using the values of the photo-generated currents, the photon flux densities, the mobilities and the other circuit quantities in relation (80) gives the effective excess carrier lifetime in the entire sample. The variation of the incident flux density with the illumination wavelength also affects the photo-response of the samples as we will see later.

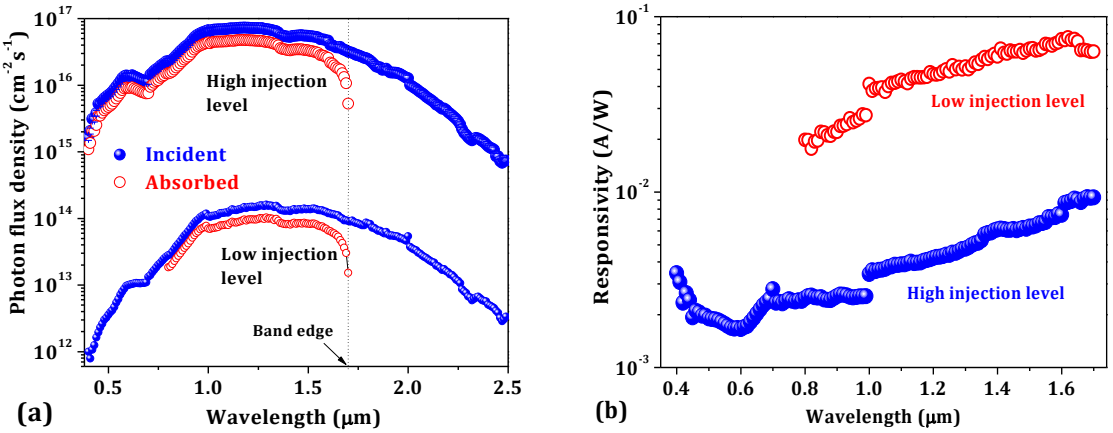

Figure 5: The spectral dependence of low injection level and relatively high injection level (a) incident and absorbed photon flux densities for p-type GaSb epilayer with room temperature carrier concentration 10^{17} cm^{-3} and mobility 700 cm^{2}V^{-1}s^{-1} and (b) responsivity of the photo-detectors for the incident photon flux density.

Figure 6 describes, the spectral dependence of low injection level (red symbols) and relatively high injection level (blue symbols) (a) photo generated current and (b) excess carrier lifetimes for the sample discussed in Figure 5. The first interesting result is the sensitivity of the signal-current and the measured excess carrier lifetimes to the photon flux density. The signal-current increases with increasing photon flux density. The excess carrier lifetime is displaying a distinctive decrease with increasing photon flux density.

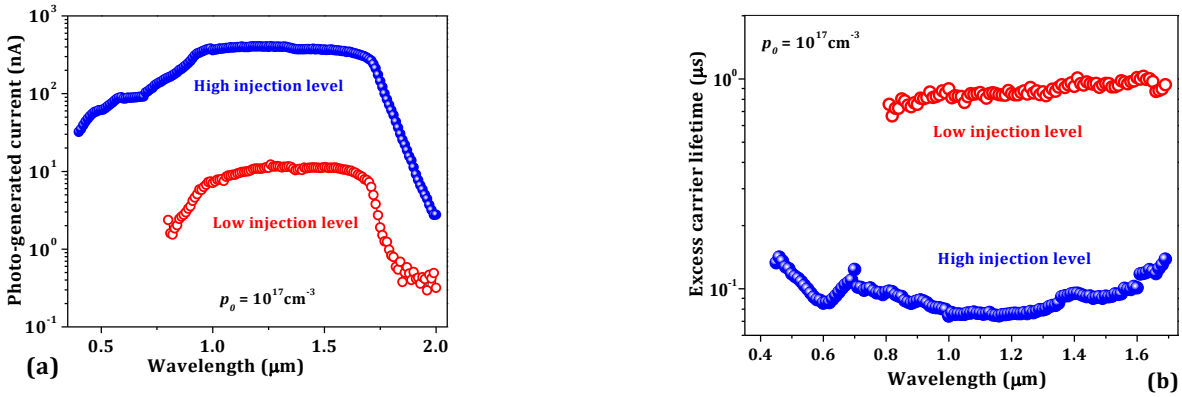

Figure 6: The spectral dependence of low injection level (red symbols) and relatively high injection levels (blue symbols) (a) photo generated current and (b) excess carrier lifetimes for the sample discussed in Figure 5.

The excess carrier lifetimes become constant at very low illumination photon flux density as shown in Figure 6 (b). The photo-response is therefore clearly non-linear for high photon flux densities, with the spectral dependence purely resulting from variations in the illumination intensity.

Figure 7 illustrates the spectral dependence of the theoretical lifetimes (labelled "τ_{eff}") fitted to the experimental room temperature values (red symbols) discussed in Figure 6 (b). The fitting can be performed for both low and high injection levels using relation (57) along with the steady-state photoconductivity measurement results in relation (80). The contributions of the under surface depletion layers 1 and 3, the deep bulk (layer 2) and the

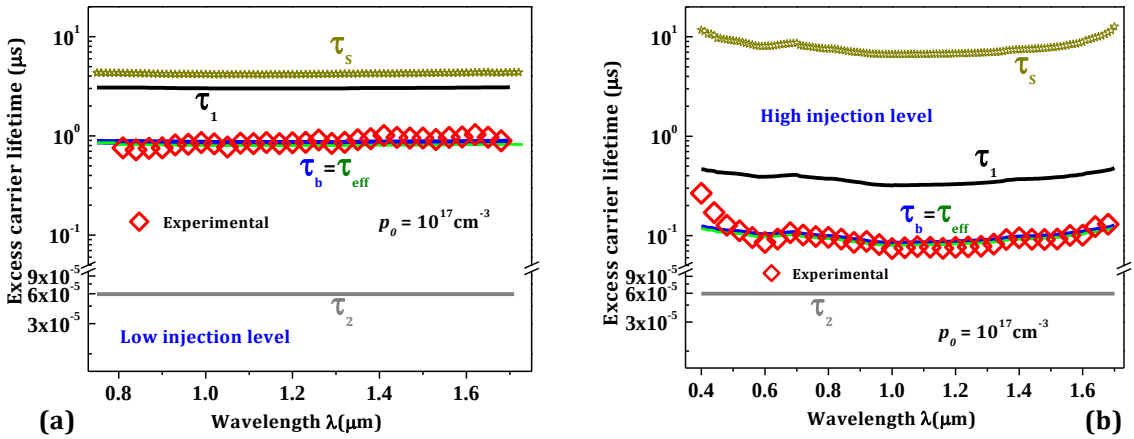

Figure 7: wavelength dependence of effective excess carrier lifetime in depletion layer and bulk of semiconductor at (a) low injection and (b) high injection level.

surface to the entire sample are also shown in Figure 7 (a) and (b). To describe the effective excess carrier lifetimes in the deep bulk, the thermal equilibrium carrier concentrations discussed in relation (7) is considered. The doping density is obtained from Hall Effect

measurements. To determine the effective excess carrier lifetimes in the entire under surface depletion layer, the thermal equilibrium carrier concentrations discussed in relation (11) is used along with the law of mass action.

The carrier recombination capture coefficients (radiative, Auger, SRH and surface) and the band bending were taken as the fitting parameters. In order to fit the experimental values, a band bending of roughly 190 meV and a value for b_1 of 50 nm are required in both the low and the high injection level cases. The surface Fermi level position also remains constant at about 290 meV above the surface valence band maximum in both cases.

According to the proposed three-layer model, the spectral ranges of the excess carrier lifetimes described in Figure 7 is limited to the low wavelength range in which the under surface depletion layers are the most dominant and the bulk excess carrier lifetime becomes spectral independent. Hence, the steady-state photoconductivity measurement result in Figure 7 (a) can be fitted using the low injection level of relation (57) when the excess carrier lifetime is independent of the incident photon flux density. The steady-state photoconductivity measurement result in Figure 7 (b), however cannot be fitted by keeping the incident photon flux density constant in the high injection regime of relation (57), and can be fitted when the spectral dependence of the incident photon flux density in Figure 5 is taken into account. This is also an evidence for the premise that the variation in the magnitudes of the excess carrier lifetime in Figure 7 (b) is purely resulting from variations in the illumination photon flux density, but not due to spectral effect.

4.3 Injection level dependence of excess carrier lifetimes

High and low injection is only meaningful when comparing the photo-generated carrier concentration and the background concentration. Conditions of high injection can occur even in heavily doped materials due to the depletion of the thermal equilibrium carrier density and the generation of excess carrier density in the depletion region as discussed earlier. As discussed earlier, the photo-generated carrier lifetime remains constant with increasing photo-generated carrier concentration under low injection and only decreases under high injection, if other properties of the samples remain constant. The photo-generated carrier concentration is however itself a function of the excitation rate. Variation in the average

excitation rate can also be caused due to a variation in the samples to samples thickness; photon flux density and the energy of illumination.

In order to describe the injection level within the optical generation-recombination region, it is advisable to relate the photo-generated carrier lifetime to the excess sheet carrier density ($b\delta n$) instead of the volume excess carrier density (δn). The variation in the energy of the illumination can affect the excess carrier lifetime depending on the doping levels of the samples and the incident photon flux density. The description of the sheet photo-generated carrier concentration dependence of the excess carrier lifetime was hence performed by varying the incident photon flux density and keeping the energy of the illumination constant. This is done again by inserting different neutral density filters.

Figure 8 illustrates the power dependence of the responsivities of p-type GaSb epilayers with various doping levels and thicknesses indicated on the graph. Drawing of Figure 8 is performed using relation (59). To obtain maximum photon flux density, the illumination of wave length 1.1 μm is used. The intensity of the incident light and the signal currents are varied by using neutral density filters. The variation in the slope of the responsivity in Figure 8 at different injection levels is mainly attributed to the contribution by different recombination mechanisms, the variations of the photo-responses within different layers in the bulk and the effects of surface recombination.

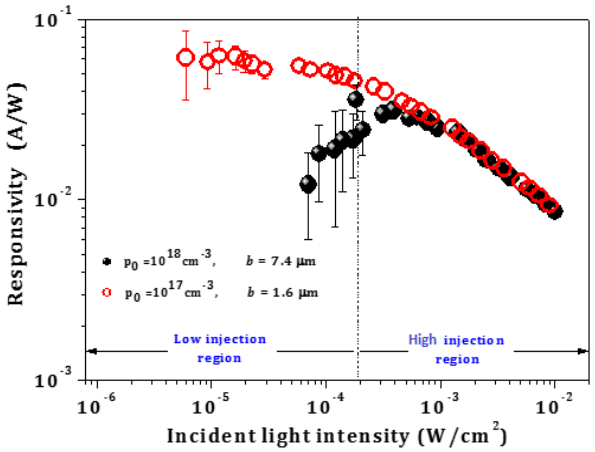

Figure 8: Power dependence of the responsivities of p-type GaSb epilayers with various doping levels.

Figure 9 shows the room temperature measurements (a) photon flux density dependence of photo-generated currents and (b) excess sheet carrier density dependences of excess carrier lifetimes for GaSb epilayers with different thicknesses and doping levels. The room temperature photo-generated current in the sample as a function of the incident photon flux density for the samples in Figure 9 (a) are determined from the photo-voltages measured using steady-state photoconductivity measurements using the circuit equation (66). The experimental results of excess carrier lifetimes represented by symbols in Figure 9 (b) are also described using relation (80). The solid lines in Figure 9 (b) represent the

effective lifetime in each sample obtained by fitting the theoretical results obtained using relation (57) to the experimental results. The band bending (E_S) at the surface, the SRH carrier lifetimes (τ_{n0} and τ_{p0}) and the surface recombination velocities (S_{n0} and S_{n0}) were also used as fitting parameters.

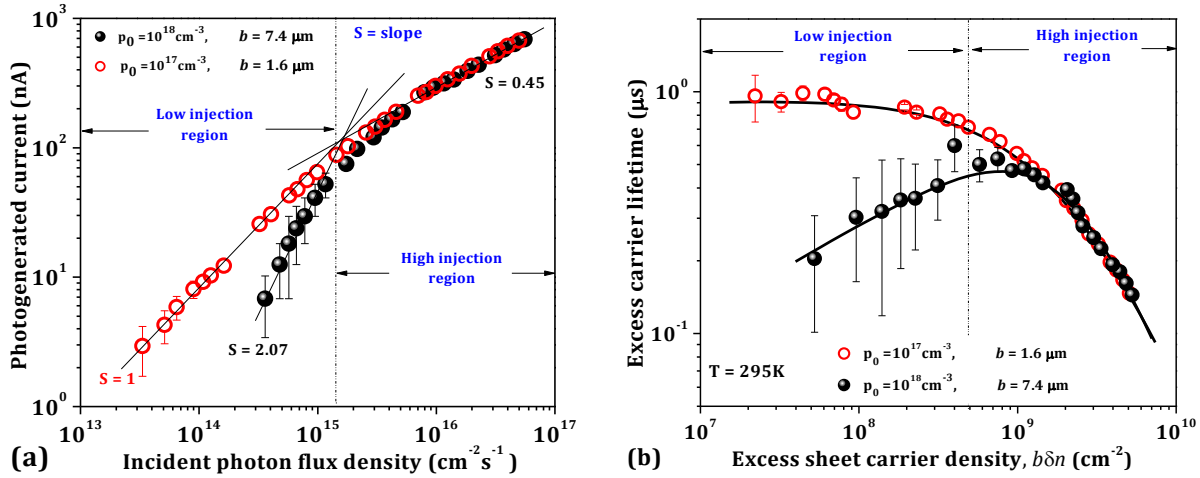

Figure 9: Room temperature (a) photon flux density dependence of photo-generated currents and (b) excess sheet carrier density dependences of excess carrier lifetimes for GaSb epilayers discussed in Figure 8.

Figure 10 depicts contributions from different regions (layer 1, layer 2, layer 3 and the surface) to excess carrier lifetimes in each sample discussed in Figure 9 (b). The contributions of layers in the bulk were determined using relations (35) to (42) for each layer and that of the surfaces were taken into account using relations (52) and (53).

The entire injection regime in each Figure 10 (a) and (b) have four different injection level regions labelled by Roman numerals I through IV. Region I is where all the layers in the bulk (layers 1, 2 and 3) are under low injection levels ($\delta n < \bar{p}_{01}$ and $\delta n < p_0$). The effective excess carrier lifetime has a maximum value dominated mostly by the contribution from layers 1 and 3, independent of the excess carrier concentration in this region and hence remains constant with increasing the injection level. Region II is where layers 1 and 3 are under high injection levels ($\delta n > \bar{p}_{01}$) and layer 2 still remains under low injection level condition ($\delta n < p_0$). The material therefore displays high injection level properties because of the dominance of layers 1 and 3 and the effective excess carrier lifetime decreases with increasing the injection level. In region III, still layers 1 and 3 are under high injection levels and layer 2 remains under low injection level condition as in region II. However, the contribution of layer 2 in the effective excess carrier lifetime becomes dominant and the effective excess carrier lifetime almost remains constant. Hence, the entire material displays

low injection level condition in region III. In region IV all the layers in the entire bulk (layers 1, 2 and 3) remain under high injection level conditions. Therefore, the effective excess carrier lifetime decreases with increasing the injection level and the entire material therefore displays high injection level condition. The experimental results of the excess carrier lifetimes are confined to regions I and II in this case. Region III and IV are not affected by recombination of carriers at the surface.

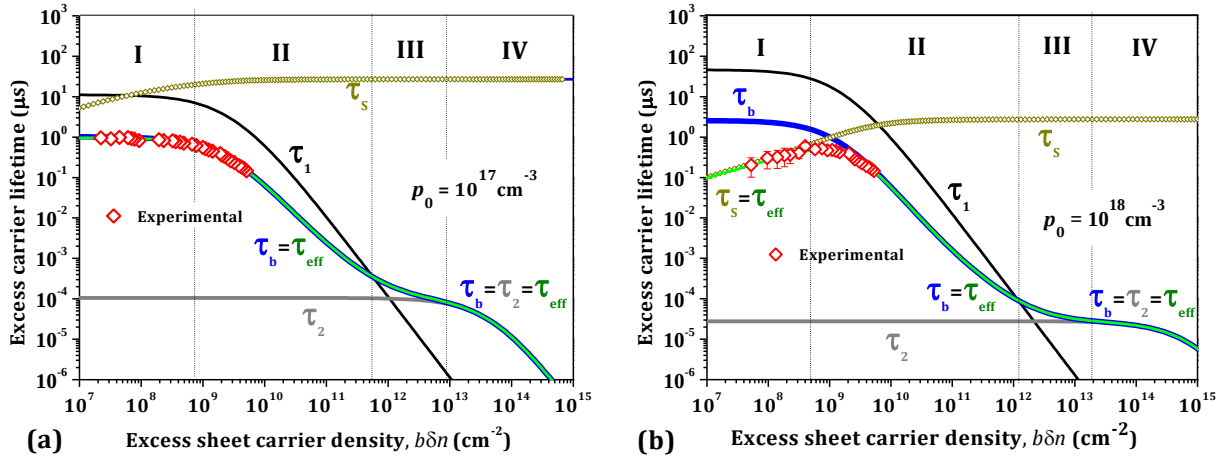

Figure 10: Contributions of different regions (layer 1, layer 2, layer 3 and the surface) to each excess carrier lifetimes discussed in Figure 9 (b).

Table 1 shows the parameters obtained in fitting of experimental and theoretical values in Figure 9 (b) and Figure 10. As can be seen the surface Fermi level positions above the VBM remains fixed with increasing the doping levels. The band bending energy at the surface increases with increasing the doping level and the width of the depletion layer decreases with increasing the doping level. As discussed in section 2.2.3, the SRH excess carrier lifetime, τ_{eff} and the surface recombination velocity, S_n are independent of the doping level, so that the variation observed in these parameters depicted in Table 1 might be attributed to the localized states in the bulk and on the surface, respectively. The surface Fermi-level position relative to the valence band maximum (VBM) obtained in this work is in complete agreement with the reports of Viljoen et al. [53] on the electronic properties of cleaved (110) surfaces obtained from photoemission measurements for the surface of a p-type GaSb. This report shows that, the surface Fermi-level for GaSb is pinned below the mid gap irrespective of the doping level of the sample. M. W. Shura *et al.* [54] also reported in their work on the two- layer model used in the description of Photoconductivity of both p-type and n-type GaSb epilayers that, the surface Fermi-level is pinned approximately at 300 meV above the

VBM. The estimated surface recombination velocities agree with the wide range of values reported by several authors (ranging from 100 cm/s to 10^6 cm/s for p-type GaSb surfaces under different conditions) [55 - 57].

Table 1: Parameters obtained in fitting of experimental and theoretical values in Figure 9 (b) and Figure 10.

No	N_a (cm^{-3})	E_S (meV)	b_1 (nm)	τ_{eff} (μs)	S_n (cm/s)	E_{SF} (meV)
1	10^{17}	210±10	30±5	≥ 80	≤ 850	290±10
2	10^{18}	250±10	18±5	≥ 120	≤ 12,0000	293±10

Figure 11 illustrates the theoretical simulation of injection level dependence of the room temperature excess carrier lifetimes (a) in the under surface depletion layers and (b) in the deep bulk of a GaSb epilayers used to describe the fittings in Figure 10 (a). All the expressions displayed in relations (35) to (57) were involved to describe both Figure 11 (a) and (b). To describe the excess carrier lifetimes in the under surface depletion layers, p_0 in relations (35) to (57) is exchanged by $\bar{p}_{01}$. The depletion of majority carriers leads to very high radiative and Auger excess carrier lifetimes in both layers in layers 1 & 3 as compared to layer 2 as shown in Figure 11 (a) and (b). As it can be seen from this figure, layers 1 & 3 are under low injection below the injection level 6.43×10^{14} cm^{-3}, and layer 2 is under low injection level below the injection level 10^{17} cm^{-3} where the corresponding excess carrier lifetimes in each layer remain constant.

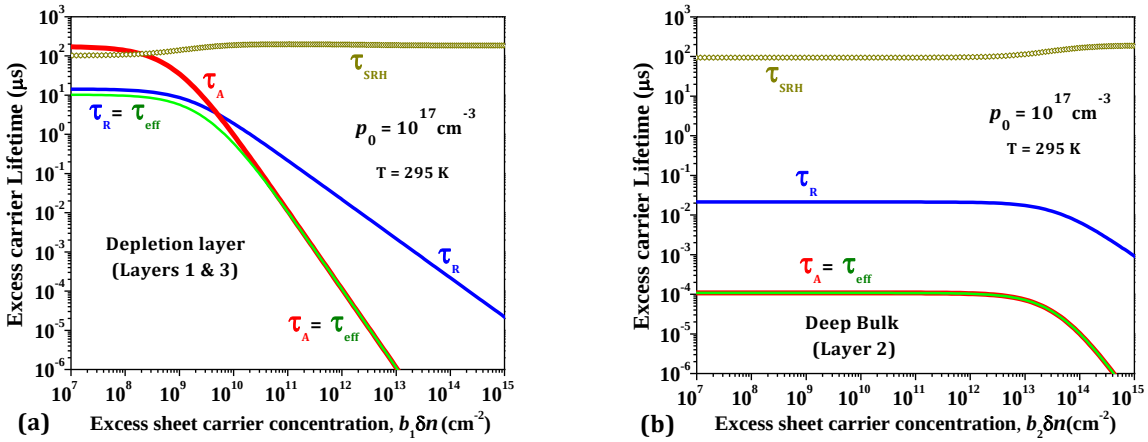

Figure 11: Theoretical Simulation of injection level dependence of the room temperature excess carrier lifetimes (a) in the under surface depletion layers and (b) in the deep bulk of a GaSb epilayers.

Auger recombination rate is seen to dominate the entire bulk at high injection levels while radiative recombination rate dominates only the low injection level of the under surface depletion layers (layers 1 and 3). Hence, in p-type samples where Auger

recombination is highly dominant in layer 2 and the surface recombination effect is negligible as the one in Figure 10 (a), the contribution of layer 2 becomes negligible and the under surafce region becomes dominant at very low injection level. The low injection level entire bulk excess carrier lifetime is then dominated by only the under surface photo-response. It seems that, Shockley-Read-Hall recombination does not effect on the photo-response of direct band gap GaSb epilayers. This can be a proof for the premise that, only band to recombination mechanisms are dominant in small direct band gap semiconductors [58] Since the surface of GaSb is p-type [59-62] the strong near-surface electric field produced due to the ionization (N_a^-) in the bulk and the surface charge, electrons in layers 1 and 3 undergo drift towards the surface in p-type GaSb epilayers, whereas holes in layers 1 and 3 drift towards the bulk. The majority of electrons generated within layers 1 and 3 are therefore more likely to be captured by surface states than recombine with the low concentration of holes present in the regions. The low concentration of holes that undergo drift into layer 2 also do not affect the low injection level steady-state carrier lifetime in layer 2. For highly doped p-type samples, the stronger near-surface electric field increases the surface recombination rate of free electrons. An increase in band bending, however, tends to increase the bulk carrier lifetime due to the decrease in the majority carrier concentration in the entire layers 1 and 2 shown in Figure 10 using green lines labelled "τ_b". However, increase in electric field also increases the surface capture probability for electrons and hence decreases the effective carrier lifetime as shown in Figure 10 (b) where τ_s overlaps τ_{eff}. Thus, although the bulk carrier lifetime in the highly doped sample is higher than in the lightly doped p-type epilayers, the effective carrier lifetime can be lower for the highly doped sample due to surface recombination Figure 10 (b). It should be noted that although the carrier lifetime is expected to be highly doping dependent in p-type GaSb epilayers, the three-layer model elegantly explains the apparent insensitivity of the effective lifetime to the doping level. This result is also in complete agreement with the reports of other authors [63-66].

5.Conclusions

The excess carrier lifetime in GaSb thin film have been studied as function of wavelength of the illumination and the injection level have been studied using steady-state photoconductivity measurements. The spectral dependence of the effective excess carrier lifetime displays a distinctive decrease with increasing photon flux density. The excess carrier lifetimes also become constant at very low illumination photon flux density and varying with photon flux density at high injection level. The photo-response is therefore clearly non-linear for high photon flux densities, with the spectral dependence purely resulting from variations in the illumination intensity not due to spectral effect. The non-linear response could be successfully described by only considering the contribution of a near-surface depletion regions to the photo-response. This is possible by using the three-layer model that can describe the contributions of different layers in the entire bulk to the photo-response. The three-layer model enable us to simulate the injection level dependence of the excess carrier lifetime by varying only the band bending at the surface and the surface recombination velocity. Once the surface band bending at the surface was known from simulation of the injection dependent measurements, the contribution made by different regions within the epilayer could be described. The results obtained for the effective excess carrier in the entire sample using this method shows that, the under surface depletion layers are the most dominant and the bulk excess carrier lifetime becomes spectral independent in a system under low injection level. As the injection level increases, the effective excess carrier lifetime decreases and the deep bulk becomes dominant at very high injection level.

Due to the reduction of the band to band radiative and Auger recombination mechanisms, the probability for the dominance of the Shockley-Read-Hall and the surface recombination mechanisms in the under surface depletion layers is very high. However, the effects of Shockley-Read-Hall recombination mechanism is not observed in the simulation of the photo-responses of GaSb epilayers in this work. In a sample where the surface recombination effect is negligible, Auger recombination rate is found to be dominant in the entire bulk at high injection levels, while radiative recombination rate dominates only the low injection level of the under surface depletion layers. The contribution of layer 2 becomes

negligible and that of the under surface depletion layers becomes dominant at very low injection level.

The three-layer model proposed in this study has therefore been able to successfully describe the photo-responses of different layers in various GaSb epilayers for spectral dependence, injection level dependence, doping level dependence and photon-energies. Hence, it is anticipated to be applicable to other direct band-gap semiconductors for which the excess carrier lifetime is limited by band-to-band radiative and Auger recombination mechanisms.

References

[1] R.H.Bube, Optoelectronic properties of semiconductors, 1992.

[2] Compound Semiconductors, vol.5,pp.16, 1999.

[3] M.C. Wu and C.C. Chen, "Photoluminescence of high-quality GaSb grown from Ga- and Sb-rich solutions by liquid-phase epitaxy" Journal of Applied Physics, vol. 72, pp. 4275, 1992.

[4] D. K. Schroder, Semiconductor Material and Device Characterization, 2nd edition. Wiley, 1998.

[5] S. Bowden and R. A. Sinton, "Determining lifetime in silicon blocks and wafers with accurate expressions for carrier density," J. Appl. Phys, vol. 12, pp. 102, 2007.

[6] N. Matsuo, H. Ohno, and H. Hasegawa, "Mechanism of high gain in GaAs photoconductive detectors under low excitation," Japanese Journal of Applied Physics, Part 2 (Letters), vol. 23 , pp. 299,1984.

[7] S. M. SZE and K. N. Kwok, Physics of Semiconductor Devices Third Edition, John Wiley & Sons.

[8] N. H.C.Berge and A.Aberle., Journal of applied Physics, vol. 11, pp. 6218, 1999.

[9] J. Brody, A. Rohatgi, and A. Ristow, "Review and Comparison of Equations Relating Bulk Lifetime and Surface Recombination Velocity to Effective Lifetime Measured Under Flash Lamp Illumination", Solar Energy Materials and Solar Cell, vol.7, pp. 293,2003.

[10] MIT Spectroscopy. The Era of Classical spectroscopy. <http://web.mit.edu/spectroscopy. <http://web.mit.edu/spectroscopy/history/history-classical.html>, 2010.

[11] R. Agarwal and C. M. Lieber., Semiconductor nanowires: optics and optoelectronics.Applied physics A, vol. 3, pp. 85, 2006.

[12] L. P. Kouwenhoven, Quantized Photocurrent in a Single-Exciton Pump,Europhysics,vol.18, pp. 607,1992.

[13] R. Sinton, "Practical measurement of bulk lifetime and surface recombination by using wavelength dependence," 3rd World Conf. onPhotovoltaic Energy Conversion, vol. 1, pp. 951, 2003.

[14] D. W,L.A. and P.R.Moran, "Solid-state-electrophotographyMedical physics:Bibcode, vol. 5, pp. 23,1978.

[15] R. L. Petritz, "Theory of photoconductivity in semiconductor films," Physical Review, vol. 104, pp. 1508,1956.

[16] D. A. Neamen, Semiconductor Physics and Devices: Basic Principles, Fourth Edition, Publishing House of Electronics Industry, pp. 634,2011.

[17] Y.Arafat,F.M.Mohammedy,and M. M. Shahidul Hassan,"Optical and Other Measurement Techniques of Carrier Lifetime in Semiconductors," J. Optoelectron. Eng, vol. 2, pp. 5,2012.

[18] K. E, "The Determination of Charge-Carrier Lifetime in Silicon," Phys. Stat. Sol., vol. 9, pp. 1865 , 2008.

[19] R.S and T.Mankad, "Ingots and Blocks," Contactless Carrier Lifetime Measurement in Silicon Wafers, pp. 1-14, 2010.

[20] M. E. A. Buscema., Large and tunable photo thermoelectric effect in single-layer MoS2. Nano. Lett., 2013.

[21] V. P. Varshni, "Band-to-Band Radiative Recombination in Groups IV, VI, and III-V Semiconductors"Physica Status Solidi, vol. 19, pp. 459, 1967.

[22] I.W and S.O Kasap., Chapter 5.7 of Electrical Engineering Materpals and Devices., 1997.

[23] J. F. Roller., Contactless Spectral-Dependent Measurement of Bulk Lifetime and Surface Recombination Velocity in silicon photovoltaic materials, 2016.

[24] Z. M. F. e. al., "Photoluminescence of InSb, InAs, and InAsSb grown by organometallic vapor phase epitaxy" Journal of Applied Physics, vol. 67, pp. 7034, 1990.

[25] http://www.ElectronicMaterials.Usask.ca..

[26] B.Streetman, Chapter 4.1 of Solid-State Electronic Devices, 4th Edition, Prentice-Hall, EE 128 textbook, 1995.

[27] J. P. McKelvey, Solid-State and Semiconductor Physics, 2nd ed., Harper & Row., New York, 1966.

[28] J. Wiley & Sons, Inc, C. Kittel, Introduction to Solid State Physics, 8th ed, 2005.

[29] F. Pierret, Advanced Semiconductor Fundamentals, in Modular series on solid state devices,Adison-Wesley Publishing Company, Inc., vol. 6, 1987.

[30] L. W. BridEman, Hall Effect"The thermodynamics of Electrical Phenomena in Metals., 1934.

[31] Kittel, Charles; Herbert Kroemer., Thermal Physics (2nd Edition). W. H. Freeman. ISBN 978-0-7167-1088-2, pp. 357, 1980.

[32] C. Kittel., Introduction to Solid State Physics, 8th ed. John Wiley & Sons, Inc., 2005.

[33] V. L. BONCH-BRUEVICH, The Electronic Theory of Heavily Doped Semiconductors, Elsevici Publ. Co, New York, 1966.

[34] D.J. Fitzgerald and A.S. Grove., "Surface Recombination in Semiconductors," Surface Science., vol. 9, pp. 347,1968.

[35] N. A, Guojun Liu,* Zhipeng Wei,* Rui Deng, Xuan Fang, Xian Gao, Yonggang Zou, Mei Li, Xiaohui Ma, "Study on Neutral Sulphur Passivation of Gallium Antimonide Surface," in National Key Laboratory of High Power Semiconductor Lasers University of Science and Technology,Changchun, pp. 23,2012.

[36] H. J.R. and Dunber ,P.M., Solid State Elec., vol. 18, pp. 715, 1975.

[37] H. H.J, Semiconductors and Semimetals, Vol-Solar Cells, Academic press, 1975.

[38] D.E. Aspnes and A. A. Studna, Dielectric functions and optical parameters of Si, Ge,GaP,GaAs,GaSb,InAs and InSb from 1.5eV TO 6.0eV.Phy.Rev.B, vol. 27, pp. 985,1983.

[39] J. I. Pankove., Optical Processes in Semiconductors. Dover Publications, Inc., New York, 1975.

[40] H.S.Bowden and C., Photovoltaic Education Network, [Online]. Available: http://www.pveducation.org/pvcdrom., 2013.

[41] www.tf.uni-kiel.de..

[42] S. Sze., Physics of Semiconductor Devices, Wiley 2nd ed, New York, 1981.

[43] "S. M. Sze and K. K. Ng, " Physics of Semiconductor Devices, 2007.

[44] R. F. Pierret, Modular Series on Solid State Devices, Reading, MA: Addison-Wesley Publishing Co, vol. 1, 1983.

[45] R. Smith, Semiconductors, 2nd ed. London: Cambridge University Press, 1979.

[46] J. Okada, Effect of External Illumination on Carrier Lifetime in Semiconductors, J. Phys. Soc. Japan, vol. 14, pp. 1550,1959.

[47] J. Okada, Recombination Centers in Germanium, J. Phys. Soc, vol. 13, Japan, pp. 793,1958.

[48] N. H, C. Berge, and A. Aberle, Journal of Applied Physics., vol. 11, pp. 6218-6221, 1999.

[49] S. R.A. and A. Cuevas., Appl. Phys. Lett, vol. 17, pp. 2510,1996.

[50] M. J. Kerr, A. Cuevas, and R. A. Sinton., Generalized Analysis of Quasi-Steady-State and Transient Decay Open Cicuit Voltage Measurements, vol. 91, pp. 399,2002.

[51] J.V.Joshi, Photoconductivity:art,science and technology, 1990.

[52] M. W. Shura, V. Wagener, J. Botha and M. C. Wagener, J. Appl. Phys. pp. 113104, 2012.

[53] P. E. Viljoen, M. S. Jazzar and T. E. Fischer, Surface Science , pp. 506,1972.

[54] M. W. Shura, V. Wagener, J. R. Botha and M. C. Wagener, Physica B, pp. 1656,2012.

[55] A.W. Betti and O. V. Sulima, Semicond. Sci. Technol, pp. 184, 2003.

[56] L. M. Fraas, J. E. Avery, P. E. Gruenbaum, V. S. Sundaram, K. Emery and R. Matson, in Proceedings of the 22nd IEEE PV Specialists Conference, pp. 80,1991.

[57] O. V. Sulima and A. W. Bett, Sol. Energy Mater. Sol. Cells), pp. 533,2001.

[58] M. Z. Rahman, Modeling Minority Carrier's Recombination Lifetime of p-Si Solar Cell., 2012.

[59] R.K. Lal, P. Chakrabarti, Prog. Cryst. Growth Charact. Mater, pp. 33,2006.

[60] D. Schroder, IEEE Trans. Electron Devices, pp. 160,1997.

[61] L. M. Fraas, J. E. Avery, P. E. Gruenbaum, V. S. Sundaram, K. Emery and R. Matson., In Proceedings of the 22nd IEEE PV Specialists Conference, pp. 80,1991.

[62] P. W. Chye, T. Sukegawa, I. A. Babalola, H. Sunami, P. Gregory and W. E. Spicer, Phys. Rev. B, pp. 2118,1977.

[63] A.N. Titkov, G.V. Benemanskaya, and G.N. Iluridze, Scale time for interband Auger recombination involving aspin-orbit-split valance band p-type GaSb crystals, 1981.

[64] G. Stollwerck, O. V. Sulima, and A. W. Bett, IEEE Trans. Electron Devices, pp. 448, 2000.

[65] C. Hilsum and A. C. Rose-Innes, "Semiconducting III-V Compounds", H. K. H. (Pergamon), Ed., New York, pp. 189,1961.

[66] S. P. Svensson, D. Donetsky, D. Wang, H. Hier, F. J. Cro., G. Belenky, J. Cryst. Growth, pp. 103, 2011.